A Modular, Transistorized Controlled-Potential Coulometer

J. E. Harrar and Ervin Behrin

Lawrence Radiation Laboratory, University of California, Livermore, Calif. 94550

A controlled-potential coulometer has been designed which consists of two plug-in modules, the potentiostat and the integrator, each of which may also be used independently. The instrument is fabricated in U. S. Atomic Energy Commission standard nuclear instrument modules. The potentiostat is based on solid-state operational amplifiers and a special power booster. The instrument has an output capability of ±24 V at ±400 mA without current polarity switching, and incorporates a convenient means for gain-bandwidth shaping so that the response of the instrument may be tailored to a variety of cell systems. The integrator utilizes a high-voltage, transistorized operational amplifier and high stability passive components. Included in the readout circuit is a compact, 4-decade voltage divider, designed for use with a digital voltmeter, which permits a direct readout of the amount of substance electrolyzed in milligrams.

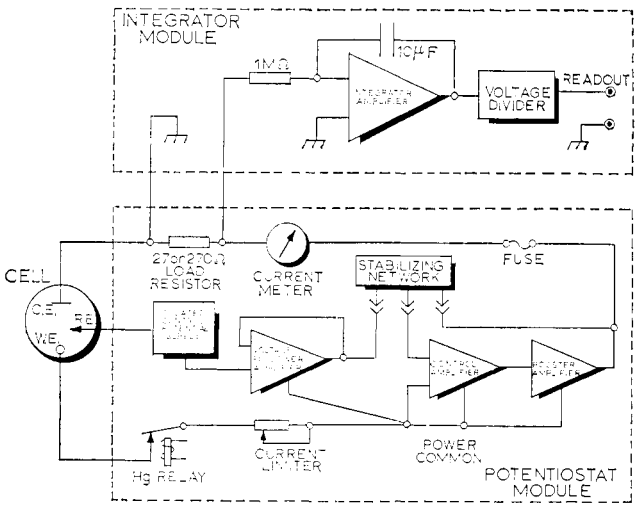

Figure 1. Controlled-potential coulometer block diagram

INCREASING INTEREST in the techniques of controlled-potential electrolysis and coulometry has produced a variety of suitable instrumentation. The wide range of apparatus is indicated by the reviews of Bard (*1*), and summaries of commercially available instrumentation have been presented by Rechnitz (*2*) and Lott (*3*). Although there are many instrument systems from which to choose, the continual improvement of electronic components and the greater understanding of how potentiostatic and coulometric circuits should function presented the possibility of a new design with still further improvements in reliability, performance, and convenience of operation.

A new instrument for controlled-potential coulometry has been designed which uses all transistorized components, makes extensive use of plug-in components for versatility and ease of servicing, and has several features of particular advantage for routine operation. The circuit design utilizes solid-state operational amplifiers in a configuration essentially the same as that described by Booman and Holbrook (*4*, Figure 19). The functions of potential control and integration have been separated into two plug-in modules which can be used independently in other types of investigations, or together as a controlled-potential coulometer. The potentiostat control circuit was designed for ease in changing its gain-bandwidth characteristics to meet varying electrolysis cell conditions, and a simple technique for testing this potentiostat for stability margin is outlined. The integrator is based on a transistorized, FET chopper-stabilized amplifier, high stability passive components, and a direct readout circuit similar to that previously reported (*5*). The performance of the instrument in several analytical determinations is presented.

DESCRIPTION OF INSTRUMENT

A block diagram of the controlled-potential coulometer is presented in Figure 1, and a complete circuit diagram is given in Figure 2, together with construction notes in Table I. The instrument was constructed in the standard chassis modules adopted by the U. S. Atomic Energy Commission Committee

Table I. Instrument Construction Notes

(see Figure 2)

1. Unless otherwise noted all plugs and jacks are mounted on module rear panels. F.P. denotes front panel
2. Potentiostat R4 and R5 are Calif. Resistor Corp. Type MCX-250. Heat sink to chassis
3. Ayrton meter shunt. Resistors R9 to R13 are selected and calibrated for meter with switch S1. Resistor values shown are approximate
4. Meter ME-1 is International Inst. Inc. (Orange, Conn.) zero center edgewise panel meter Type 1145-HC 50-dc μA with face labeled "Reduction" for forward current and "Oxidation" for reverse current
5. For independent operation of modules, power plug adaptor LRL LE-15168-41 is used
6. Normal connection for use in coulometer. Pomona Electronics Co. Model 1855 shorting bar is used
7. P2A amplifier is mounted so that its case is insulated from the chassis. Unit is positioned so that zero trim is accessible inside module
8. For all voltage follower input wiring which is active in the operate configuration, including the control potential source and reference electrode terminal wiring, use short or shielded leads. Insulate the shield from the chassis and tie it to J10
9. Integrator amplifier is positioned so that balance adjustment is accessible through hole in module panel
10. All integrator signal grounds (S GND) are tied directly to J7
11. Integrating capacitor C1 is located away from heat sources
12. Coulometer chassis power receptacle and fuse are mounted in instrumentation bin connector cover
13. Coulometer chasis connectors are located to mate with two 8-inch wide plug-in modules

(1) A. J. Bard, ANAL. CHEM., **38**, 88R (1966).
(2) G. A. Rechnitz, "Controlled-Potential Analysis," Macmillan, New York, 1963, Chap. 3.
(3) P. F. Lott, *J. Chem. Educ.*, **42**, A261, A361 (1965).
(4) G. L. Booman and W. B. Holbrook, ANAL. CHEM., **35**, 1793 (1963).
(5) F. B. Stephens and J. E. Harrar, *U. S. At. Energy Comm. Rept.* **UCRL-7165**, 1963.

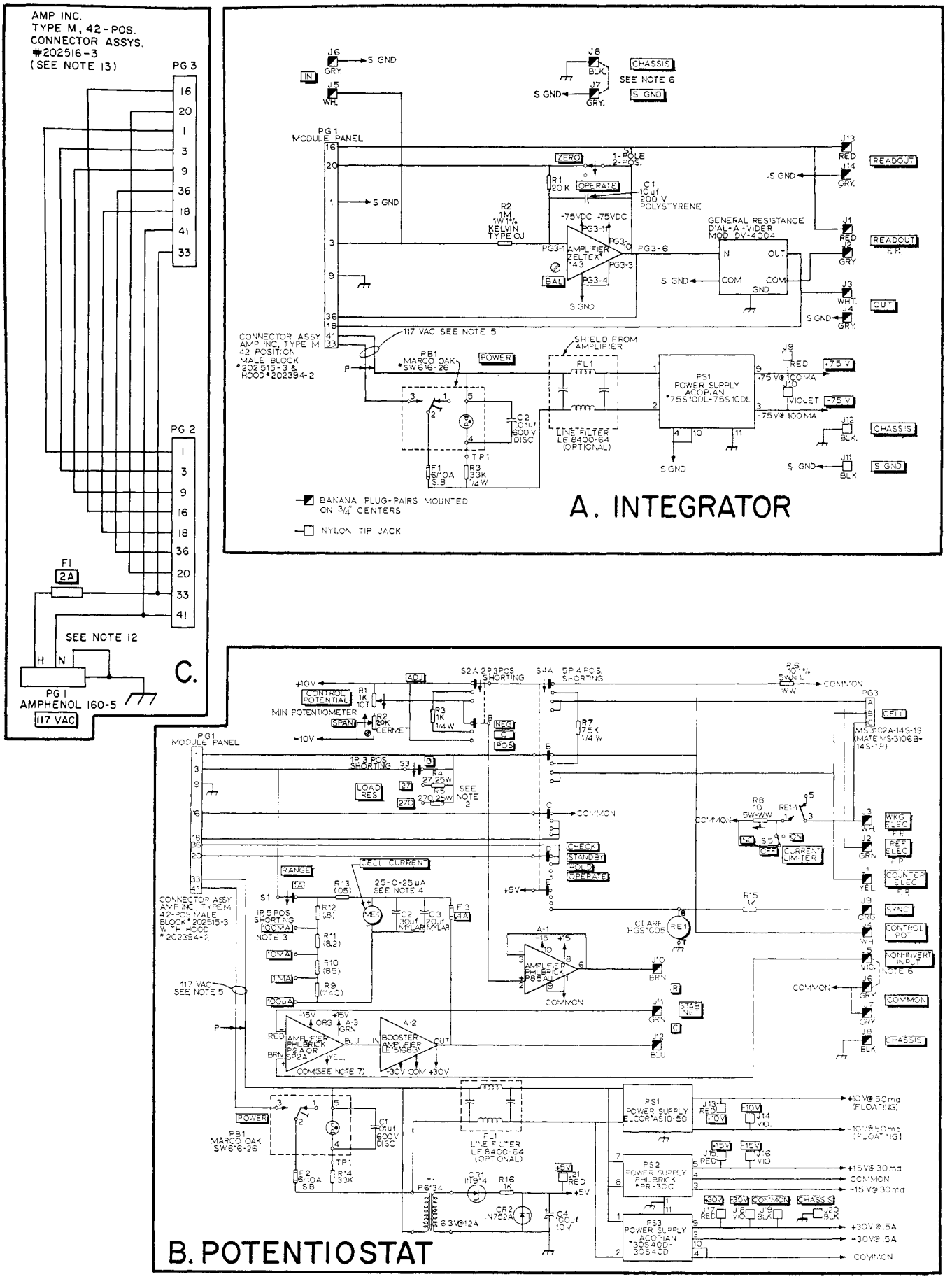

Figure 2. Controlled-potential coulometer circuit wiring diagram

on Nuclear Instrument Modules (*6*). The coulometer consists of two plug-in sections, the integrator (Figure 2A) and the potentiostat (Figure 2B), which are interconnected through wiring in the main chassis (Figure 2C). Each of these modules can also be powered and operated alone with plug adaptors; each module is provided with a number of external signal and grounding connections to permit flexibility in separate use.

Basic Circuit Configuration. Among the many potentiostatic circuit arrangements that are possible for use with an integrator, several have been devised which obviate the need for a current follower (*7*) amplifier to compensate for the effect of a current-measuring load resistor. The circuit of Kelley, Jones, and Fisher (*8*) involves a single-ended amplifier modified to operate differentially and places the load resistor in the noninverting amplifier input. Booman and Holbrook (*4*) also used a single-ended amplifier but placed the load resistor in the counter electrode circuit and isolated the power supply/amplifier common from power line/chassis ground.

The advent of stable, solid-state differential amplifiers allowed the use of the circuit of Kelley, Jones, and Fisher without isolation of the amplifier common (*5*), but this configuration is less desirable than that of Booman and Holbrook (*4*) because of complications in potential control stability when an external phase compensation or stabilizing network is used around the control amplifier. The reason for this is illustrated in Figure 3, which shows a differential amplifier with a simple, external stabilizing network consisting of an input resistor and feedback capacitor. Assuming the amplifier is operating with input voltages e_1 and e_2 appearing across impedances Z_1 and Z_2, the transfer function of the circuit in Laplace transform s-variable notation is

$$e_0 = -e_1\left(\frac{1}{RCs}\right) + e_2\left(\frac{RCs+1}{RCs}\right) \qquad (1)$$

Thus there is an unbalance in the response of the two inputs which makes closed-loop stabilization of such circuits less straightforward. Balance can be achieved by the use of identical networks in each input, but the more satisfactory arrangement used here is to operate the noninverting input at the amplifier common potential—i.e. Z_2, $e_2 = 0$. The amplifier common is in turn connected to the working electrode. This necessitates placing the current-measuring resistor in the counter electrode lead as shown in Figure 1.

Because it is desirable to have the integrator and its readout device referenced to chassis ground, this circuit (Figure 2A) is connected to chassis ground at J7, J8. The potentiostat common (Figure 2B) is isolated from the chassis for use in the coulometer, and the counter electrode side of the load resistor is connected to chassis ground through the integrator module (Figure 1). Both the reference and working electrodes are thus floating with respect to chassis ground.

Potentiostat. The source of control potential (PS 1, Figure 2B) is an Elcor Inc. (Silver Spring, Md.) 10-V, 50-mA isolated, zener-regulated power supply. The dc output of this power supply in the potentiostat circuit has less than 0.02% peak-to-peak ripple. A fraction of this voltage is selected by adjustment of the miniature span potentiometer mounted on the rear panel, and this voltage becomes the full-scale voltage of the control-potential-adjust potentiometer.

(6) L. Costrell, *U. S. At. Energy Comm. Rept.* **TID-20893** (*rev.*), 1966.
(7) W. M. Schwarz and I. Shain, ANAL. CHEM., **35**, 1770 (1963).
(8) M. T. Kelley, H. C. Jones, and D. J. Fisher, ANAL. CHEM., **31**, 488, 956 (1959).

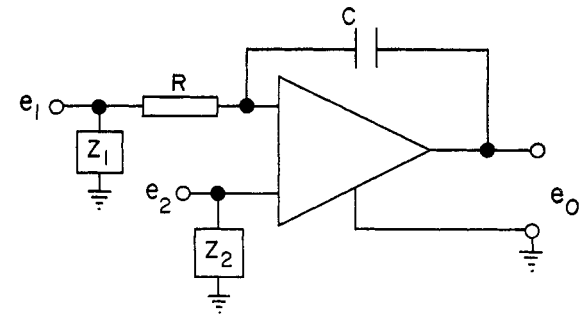

Figure 3. Differential amplifier with stabilizing network

The zero position of the control potential polarity switch disconnects the control potential supply circuit from the potentiostat and obviates resetting the control-potential-adjust potentiometer to zero during potentiostat zero offset checking.

The voltage follower amplifier (A-1, Figure 2B) is a Philbrick Researches (Dedham, Mass.) Model P85AU operational amplifier, specified as having a dc input impedance as a follower of 88 MΩ. The voltage follower provides isolation between the reference electrode impedance and the control amplifier with its stabilizing network. The control amplifier (A-3) is a Philbrick Model P2A operational amplifier. The recently introduced, lower cost Philbrick P2AU amplifier would also be suitable for the control amplifier. Power for both the P85AU and the P2A amplifiers is supplied by a Philbrick Model PR-30C power supply. The connection from the noninverting input of the control amplifier to the power common is made externally at the rear panel (J5, J6, Figure 2B) so that, if desired, an additional bias such as a scan voltage may be inserted at this point.

The control amplifier drives a booster amplifier (A-2, Figure 2B) which provides up to ±24 V and ±400 mA output. A complete schematic of the booster amplifier is shown in Figure 4. Transistors Q1 through Q4 constitute the input section with Q1 and Q3 providing two stages of amplification for positive signals and Q2 and Q4 similarly amplifying negative signals. R1, R2, and C1 shape the input impedance, with CR1 and CR2 providing overload protection. The dc input impedance of 61 kΩ minimizes loading and prevents excessive degradation of the dc open-loop gain of the control amplifier. Current amplification is provided by Q5 and Q7 for positive signals and Q6 and Q8 for negative signals, with both circuits acting as emitter followers. Quiescent current through the output stage is 50–100 mA. The dc offset of the booster is minimized by adjustment of potentiometer R8. However, because the effect of the booster offset on the total potentiostat offset is reduced by the dc open-loop gain of the control amplifier, adjustment of the offset to within ±0.1 V is sufficient.

Except for the output transistors Q7 and Q8 which are bolted to the main chassis, the booster is fabricated on a 8- × 10-cm printed circuit board. The booster is powered by a plug-in, dual output Acopian Corp. (Easton, Pa.) power supply. Construction of the potentiostat with an easily replaced booster and power supply permits simple modification of the output characteristics by installation of other types of boosters.

The frequency response characteristics of the booster amplifier were designed to match those of the control amplifier so that a maximum open-loop gain-bandwidth could be achieved in the potentiostat with a minimum of complication in its stabilization for closed-loop operation. Because the sub-

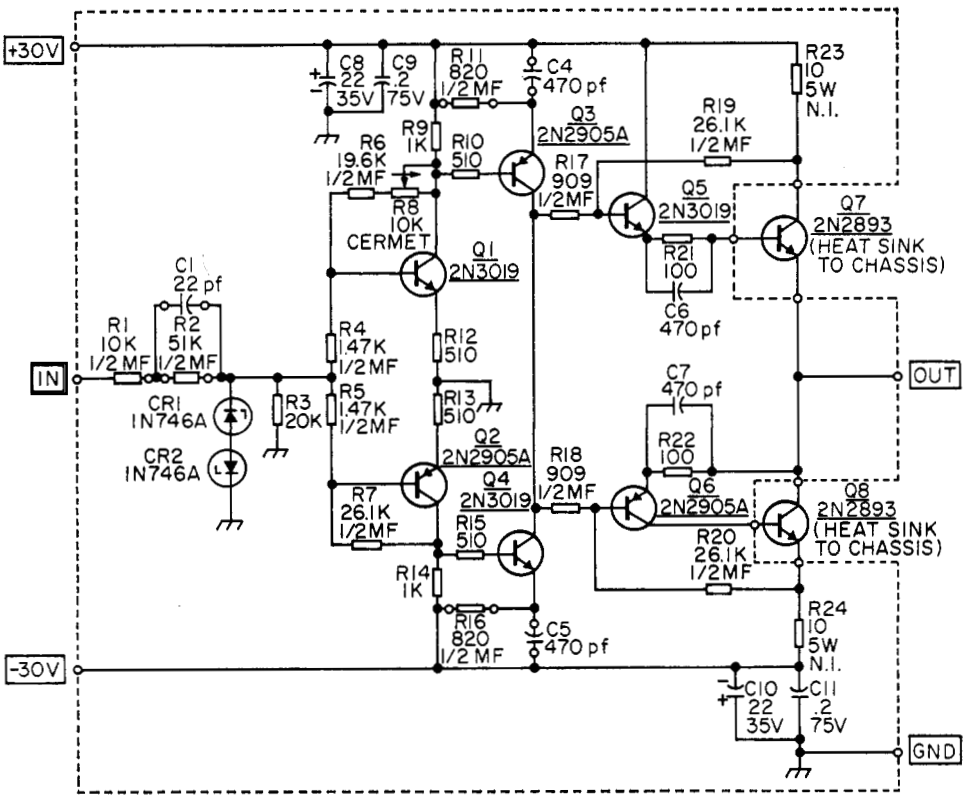

Figure 4. Potentiostat power booster amplifier wiring diagram

NOTE:

1. **Booster ground to be floated from potentiostat chassis**
2. **—○— indicates solder post on P.C. board**
3. **C-2, C-3 not used**
4. **If quiescent current exceeds 60 mA, increase R19, R20 to 28.7 K**

merged pole (*9*) of the P2A amplifier is located at a gain of 0.3–0.4, the booster voltage gain was adjusted to about 3 so that excessive phase shift from the P2A would not be introduced into the overall circuit. In addition, the gain of the booster was designed to be flat within 1 dB, with negligible phase shift, up to 100 kHz for resistive loads greater than 25 Ω.

Stabilization of the amplifier-booster system for various external loads is accomplished by means of stabilizing networks installed around both the P2A and the booster, as shown in Figure 1. The appropriate stabilizing network is assembled in a Pomona Electronics Co. (Pomona, Calif.) Model 2095 component mounting box and plugged into the rear panel of the potentiostat (J10, J11, J12, Figure 2B).

The current delivered by the potentiostat is indicated by an edgewise, zero-center meter with an Ayrton-type shunt. The zero-center meter, together with the bidirectional current capability of the booster, eliminates the need for operator anticipation of the direction of current flow. This characteristic is often important during background current investigations; it obviates potentiostat switching during analyses involving successive oxidations and reductions; and it is useful during determinations of formal potentials of redox couples. The meter and shunt are bypassed with 50-μF capacitance to reduce their contribution to the feedback loop attenuation characteristics at higher frequencies. Output short-circuit protection is afforded by a fuse in the output lead.

The working electrode is connected to the amplifier common through a current limiter rheostat (R8, Figure 2B), which is useful for limiting the cell current without manipulation of the control potential potentiometer. The *iR* drop in the current limiter resistor causes the working electrode potential to be less cathodic in the case of a reduction process or less anodic in the case of an oxidation process than the control potential. This current limiter is effective only at current levels above about 5 mA; during electrolyses involving a decay of the electrolysis current, the resistor is set to limit the initial current, and the working electrode potential automatically approaches the control potential as the cell current decreases.

The potentiostat load resistors (R4, R5, Figure 2B), from which the integrator derives its input signal, are California Resistor Corp. (Santa Monica, Calif.) high stability units rated at 0.05% resistance change per 1000 hours of operation.

Integrator. The integrator input resistor (R2, Figure 2A) and feedback capacitor (C1) also were chosen for their stability. The Kelvin Co. (Van Nuys, Calif.) resistor is specified as 0.003% drift per year. Polystyrene capacitors, which are rated at less than 0.1% drift per year, are available from Electronic Associates (Long Branch, N. J.) and Southern Electronics (Burbank, Calif.).

The ouput of the integrator appears across a General Resistance, Inc. (New York, N. Y.) Dial-A-Vider voltage divider. No stability specification is available for this component, but its accuracy is given as ±0.004%. With an appropriate setting of the four thumbwheel switches of the Dial-A-Vider and with the potentiostat 27-Ω load resistor, a direct readout in mg of the amount of material electrolyzed can be obtained. With the 270-Ω load resistor, the readout

(9) G. A. Korn and T. M. Korn, "Electronic Analog and Hybrid Computers," McGraw-Hill, New York, 1964, pp. 153–7.

voltages correspond to 10 times the quantity of substance electrolyzed. The direct readout feature is especially convenient when the readout voltages are measured with a high-resolution automatic device such as a digital voltmeter. The voltage divider factors are calculated from the instrument calibrations and the applicable electrochemical equivalents. The integrator amplifier is a Zeltex, Inc. (Concord, Calif.) Model 143 plug-in operational amplifier which has an output rating of ±50 V. The full-scale integrator ranges corresponding to the 27-Ω and 270-Ω load resistors are 19 and 1.9 coulombs, respectively. Integrator offset and drift are adjusted by means of an amplifier-mounted potentiometer which is accessible through a hole in the integrator module front panel. The amplifier is operated by a dual-output Acopian power supply.

A number of integrator circuit test points are brought out to rear-panel banana jacks for checkout and flexibility in application as shown in Figure 2A. The circuit is wired independently of chassis ground, and signal ground is connected to chassis ground externally at J7, J8 (see Figure 2A) for use with readout instruments which are referenced to chassis ground. A zero-operate switch is provided which discharges the integrating capacitor and opens the circuit for integration; this switch duplicates one function of the potentiostat control switch and is particularly useful for maintaining the integrator at zero during preelectrolysis steps.

Controlled-Potential Coulometer Operation. When the potentiostat is switched to check, the circuit feedback loop is closed and connected internally to a 10-Ω load resistor connected to the circuit common (S4, R6, Figure 2B). A current can be delivered to this load resistor by adjustment of the control potential potentiometer, and is utilized for testing the output capability of the potentiostat and for checking the meter calibration. With a zero setting of the control potential, the meter indicates the zero offset of the potentiostat; a 100-μA current reading corresponds to 1-mV offset. The voltage applied to the load resistor also appears at jack J4 on the rear panel of the potentiostat where it may be measured for verification of the control potential dial calibration. This voltage also appears directly on the readout device when the potentiostat is used with the integrator module.

By virtue of wiring between the potentiostat and integrator modules, the integrator capacitor is shorted in both the check and standby configurations of the potentiostat. In standby the potentiostat feedback loop is floating and closed through a 75-kΩ resistor.

In the hold position of the potentiostat control switch, the circuit is connected to both the counter and reference electrode terminals, and the integrator condition is determined by its zero-operate switch.

When the potentiostat is switched to operate, the mercury-wetted contact relay is energized, connecting the working electrode terminal to the circuit common, and current flow to the external circuit is initiated. The 5-V signal which energizes the relay also is brought out to the rear-panel sync jack (J9, Figure 2B) where it may be used to trigger an oscilloscope for observation of the initial current transient. Conversely, the potentiostat may be operated remotely by application of a 5-V, 1.5-mA signal to this jack. Switching of the instrument first to the counter and reference electrodes with a shorting switch (keeping the feedback loop closed) and then connecting the working electrode to the circuit with a mercury relay is a procedure which provides an electrically smooth transition from the standby configuration to operation with the cell.

EXPERIMENTAL

Frequency Response Measurements. The steady-state, gain-frequency characteristics of the potentiostat, its components, and cells were measured with a Hewlett-Packard (Palo Alto, Calif.) Model 310A and a Quan-Tek Laboratories (Whippany, N. J.) Model 304 wave analyzer. Signal magnitudes in the range of 0.3–200 mV were employed.

Transient Response Measurements. The square-wave response of the potentiostat–cell system was obtained by connecting the output of a Hewlett-Packard Model 3300A function generator through a 100-kΩ resistor to the inverting input of the P2A amplifier (J11, Figure 2B). The function generator was floated from power line ground with an Elcor Model L131 isolation transformer. The output ground of the function generator was then connected to the potentiostat common terminal.

The system response to the inserted square wave was observed with a Tektronix (Beaverton, Ore.) Type 564 oscilloscope and the signal traces were photographed with a Beattie Coleman (Anaheim, Calif.) Model FP-K5 camera. Depending on the particular cell characteristics and system wiring, varying amounts of hum and noise are observed at the controlling reference electrode which may partially obscure the system square-wave response. To avoid this and possible voltage follower input loading errors, the actual response at the working electrode as a measure of system stability thus is best obtained by measurement at a second reference electrode which is independent of the potentiostat. Both reference electrodes used were Beckman No. 39178 fiber-junction calomel probes.

The oscilloscope was equipped with a Tektronix Type 3A3 differential amplifier and matched Type P6023 adjustable 10× probes. Nonattenuating probes may also be used for measurements with the auxiliary reference electrode. However, it is important to use matched probes and amplifier inputs in this type of measurement because several volts of common mode hum signal may be present at the working and reference electrodes. The frequency of the square wave was low enough so that the transient response to each step died out before the next transient began—i.e., the waveform was still recognizable as a modified square wave. For the coulometric type cells tested in this work, a frequency of 30 Hz was found to be satisfactory.

The potentiostat output voltage overload characteristic was determined by connecting the oscilloscope to the booster output (J12, Figure 2B) and to the common terminal. The oscilloscope sweep was triggered by the 5-V step appearing at the sync jack (J9, Figure 2B) when the instrument was switched from hold to operate.

Calibration. The controlled-potential coulometer was calibrated electrically by using the potentiostat as a precision constant current source (*8*). Electro Scientific Industries (Portland, Ore.) Type SR1 precision resistors were connected between the counter and working electrode terminals and a 1.3-V mercury battery was connected between the counter and reference electrode terminals. With the instrument switched to operate, the current flowing into the integrator was calculated from the voltage drop across the precision resistor measured with a Rubicon (Philadelphia, Pa.) Model 2700 potentiometer. With the readout Dial-A-Vider set to 0.5000, the time required for the readout voltage to change from 0.500 to 11.50 V was measured with a Standard Electric Time Co. (Springfield, Mass.) Type S-100 timer. The readout voltages were measured with a Non-Linear Systems (Del Mar, Calif.) Type 484A digital voltmeter. A Leeds & Northrup (Philadelphia, Pa.) Model W 1-mV full-scale recorder was used to determine the drift rate of the integrator. This test is carried out by placing the potentiostat control switch in hold, the integrator switch in operate, and measuring the readout at the maximum Dial-A-Vider setting. The feedback loop between the counter and reference electrode terminals should be closed during this test.

Analytical Determinations. APPARATUS. The mercury pool electrode cell assembly was similar to the large cell described by Jones, Shults, and Dale (*10*), with the addition of a double-oblique-bore Teflon-plug stopcock sealed to the bottom of the cell for solution drainage and introduction of mercury. The area of the mercury pool in this cell was 11 cm^2 and the solution volume was 6 ml. The platinum gauze electrode cell has been described in detail previously (*11*). All volumetric glassware was certified or recalibrated before use.

REAGENTS. Deionized water was used for the preparation of solutions. Stock solutions of gold and lead were prepared from 99.95% and 99.999% purity metals, respectively. NBS primary standard U_3O_8 was used for the uranium standard solutions. Eastman No. 497 thiourea was recrystallized once from water. All other chemicals were reagent grade. Solutions electrolyzed in the mercury cell were deaerated with high purity nitrogen.

PROCEDURES. Micropipets were used for taking aliquots of the standard solutions for analysis. Gold was determined by reduction of Au(III) to the metal on a platinum electrode at +0.48 V *vs.* SCE in 0.5*M* HCl (*12*). The electrolysis was terminated with the current reached 25 μA. The gold was removed from the electrode by polarization at +1.0 V *vs.* SCE in 2.0*M* HCl. Lead was determined by reduction to Pb(Hg) at −0.55 V *vs.* SCE in 1.0*N* $HClO_4$ (*13*). The solution was preelectrolyzed at −0.10 V *vs.* SCE until the current reached 15 μA, and the lead electrolysis was terminated at 25 μA. Thiourea was determined by oxidation to formamidine disulfide on a platinum electrode at +0.65 V *vs.* SCE in 0.05*M* H_2SO_4 (*14*), and the electrolysis was terminated when the current reached 100 μA. The uranium solutions were analyzed by reduction of U(VI) to U(IV) in 0.5*M* H_2SO_4 at a mercury electrode potential of −0.30 V *vs.* SCE (*15*). The solution was preelectrolyzed at +0.10 V *vs.* SCE until the current reached 5 μA. For the high-level uranium determinations the reduction was continued until the current reached 10 μA; for the low-level uranium solutions each electrolysis was carried out for 10 minutes, with the final current varying from 3 to 5 μA. Background corrections were determined by electrolysis of the supporting electrolytes by the same procedures and for the same lengths of time as were required for the analysis of the samples.

INSTRUMENT PERFORMANCE AND DISCUSSION

Potentiostat. Figure 5 shows the basic open-loop gain-frequency response of the potentiostat, together with the circuit used to obtain it. The measurement technique involving the use of wave analyzers was similar to that used by Booman and Holbrook (*4*). A minimum stabilizing network consisting of a 1000-Ω input resistor and a 200-pF feedback capacitor was installed for these measurements.

Because the potentiostat was designed principally for use with large scale electrolysis apparatus, the very high gain and wide bandwidth possible with several other operational amplifiers were not required. The instrument thus is not recommended for use in fast response kinetic studies at microelectrodes. For application to coulometric and electrodeposition type cells, the basic open-loop gain-frequency characteristic of the instrument, Figure 5, must usually be modified considerably to achieve stability. The function of the basic open-loop response then becomes one of activating the stabilizing network so that the effective open-loop response of the potentiostat is reasonably predictable from the parameters of this passive network.

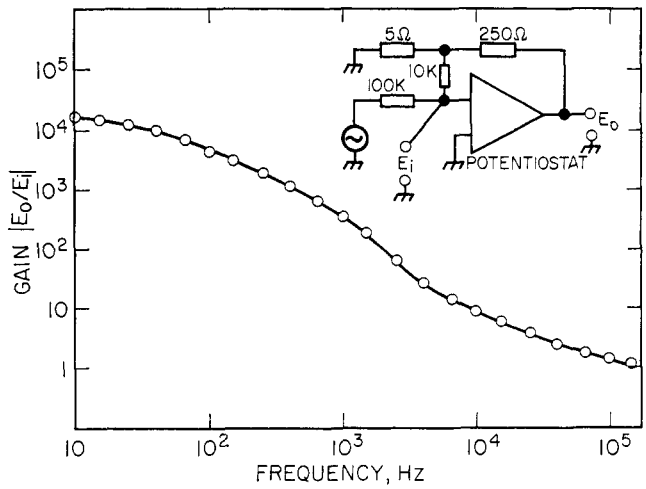

Figure 5. Potentiostat open-loop, gain-frequency characteristic

The selection of the proper stabilizing network for a particular cell-potentiostat system can involve varying degrees of empiricism. The most completely quantitative approach is to carefully measure the cell parameters or cell transfer function, and then fit the characteristics of the control circuit so that optimum system response is obtained. The rationale and methodology of this approach is described in detail by Booman and coworkers (*4*, *16–18*). Such procedures are almost mandatory when maximum bandwidth must be conserved and meaningful fast-rise response across the double layer is desired. These steady-state transfer function methods are also useful for large-scale electrolysis experiments (*4*), but are somewhat disadvantageous for routine use in analytical coulometry, because the cell and control circuit transfer functions may vary significantly with factors that are not carefully controlled. For example, the system transfer functions will be influenced to some extent by the level of faradaic current (*16*) and by the amount of series resistance placed in the loop by the current-measuring resistor and the meter circuit. Moreover, a single optimum stabilizing network may be difficult to find for analytical determinations which involve a successive oxidation and reduction at widely different potentials.

Regardless of the procedure used for arriving at a suitable stabilizing network, the system operation must be observed experimentally by observing the steady-state potential between the reference and working electrodes with an oscilloscope. However, the inadequacy of this technique is that no indication of the stability margin is obtained, and no knowledge is gained of how the potential control follows disturbances.

The procedure found suitable for final stability checks on the potentiostat described here is to monitor the response of a given cell–potentiostat system to an impressed square wave.

(10) H. C. Jones, W. D. Shults, and J. M. Dale, ANAL. CHEM., **37**, 680 (1965).
(11) J. E. Harrar and I. Shain, *Ibid.*, **38**, 1148 (1966).
(12) J. E. Harrar and F. B. Stephens, *J. Electroanal. Chem.*, **3**, 112 (1962).
(13) P. R. Segatto, *J. Am. Ceram. Soc.*, **45**, 102 (1962).
(14) K. S. V. Santhanan and V. R. Krishnam, *Z. Physik. Chem. (Frankfurt)*, **34**, 312 (1962).
(15) G. L. Booman, W. B. Holbrook, and J. E. Rein, ANAL. CHEM., **29**, 219 (1957)
(16) G. L. Booman and W. B. Holbrook, *Ibid.*, **37**, 795 (1965).
(17) D. T. Pence and G. L. Booman, *Ibid.*, **38**, 1112 (1966).
(18) I. Shain, J. E. Harrar, and G. L. Booman, *Ibid.*, **37**, 1768 (1965).

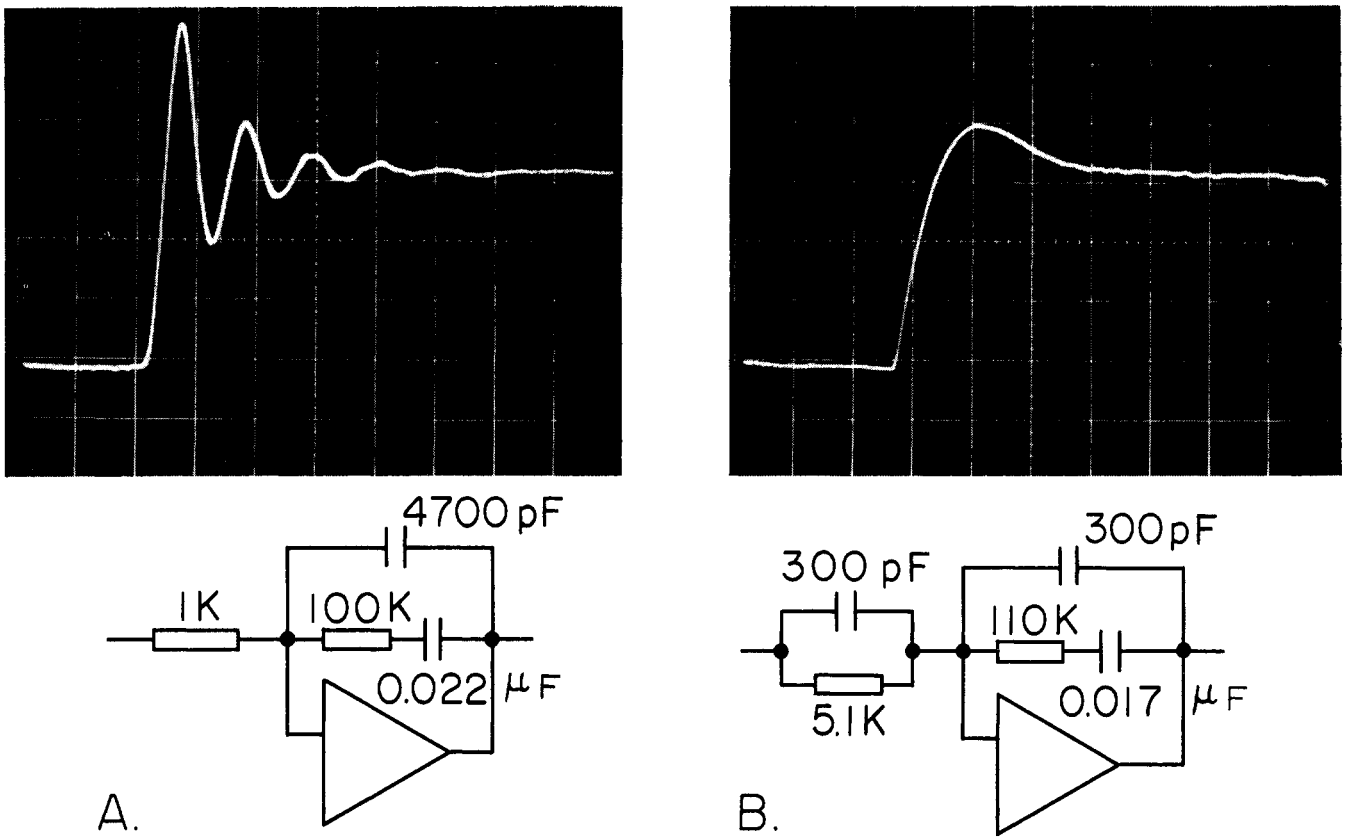

Figure 6. Transient response of potentiostat-cell system with two different stabilizing networks

Vertical scale: 20 mV/division
Horizontal scale: 2 milliseconds/division
Mercury pool cell, $E = -0.30$ V *vs.* SCE, 0.05*M* H_2SO_4

The system transient response indicates directly the important time domain parameters such as magnitude of peak overshoot and settling time. This information can be correlated with the system gain and phase margin and can be used to verify predictions based on previously measured or calculated cell and potentiostat frequency response characteristics (*19*). Alternatively, if a stable cell-potentiostat system can first be obtained, the potentiostat can be optimized for a particular cell by trial-and-error adjustment of the stabilizing network, without prior knowledge of the cell characteristics. This empirical procedure can be implemented by connecting R-C substitution boxes in place of the plug-in stabilizing network. An advantage of the square-wave response method is that the results of a change, either in the cell or in the network, are quickly available. Variations in stability caused by changes in faradaic current level and dc applied potential are readily apparent.

An example of the use of the square-wave response observation is shown in Figure 6. The electrolysis conditions were those of the coulometric determination of uranium. The photographs were taken with blank solutions in the cell; slightly greater damping was observed at faradaic currents of 50-100 mA. Figure 6A shows a greatly underdamped system, while Figure 6B is much more satisfactory. Both of these networks produce a flat response region in the potentiostat from about 100 Hz to 1 kHz; the principal difference in the two is the gain in this region, 100 for circuit A and 22 for circuit B. The function of the picofarad capacitors is to tailor the higher frequency gain for stability in the standby and hold configurations of the instrument. Open-loop, steady-state frequency response measurements have also been made on several systems, and good agreement has been found between the calculated closed-loop response and the observed square-wave response. For example, measurements on the system of Figure 6B yield a calculated system crossover frequency (*17*) of 200 Hz and an estimated time to reach peak overshoot (*20*) of 2.5 milliseconds, close to the observed value. Network B has been found satisfactory for the entire potential range in 0.05–1.0*M* H_2SO_4 and $HClO_4$ in the mercury pool cell.

The stabilizing network used for the platinum gauze electrode cell in the region of +0.50 V *vs.* SCE with 0.05–1.0*M* HCl, H_2SO_4, and $HClO_4$ consists of a parallel, 5.1-kΩ 750-pF input impedance, together with a 400-pF feedback capacitor. This network produces a steady rolloff of 6 dB per octave in the potentiostat response in the region of the cell–potentiostat crossover, up to about 30 kHz where a slight boost is introduced by the 750-pF capacitor. The great contrast between the optimum stabilizing networks for the mercury and platinum electrode cells is due to a significant difference in the cell attenuation characteristics. This is apparent from transfer function measurements which show that the mercury cell has a greater than 6 dB per octave rolloff from a low initial attenuation, whereas the platinum cell has a large low-frequency attenuation with only a slight rolloff in the crossover region.

(19) H. Chestnut and R. W. Mayer, "Servomechanisms and Regulating System Design," Vol. I, 2d ed., Wiley, New York, 1959, Chap. 15.

(20) *Ibid.*, p. 507.

Table II. Analyses with Controlled-Potential Coulometer

Substance determined	Working electrode	Background correction, mg	Taken, mg	No of determinations	Found, mg	Rel. error, %	Rel. std. dev., %
Au	Pt	0.004	4.957	5	4.953	−0.08	0.03
Pb	Hg	0.008	6.221	5	6.214	−0.12	0.06
Thiourea	Pt	0.004	5.304	6	5.281	−0.44	0.06
U	Hg	0.006	4.922	5	4.918	−0.08	0.05
U	Hg	0.003	0.3687	5	0.3697	+0.27	0.28

Maintenance of smooth potential control at all times during an electrolysis requires transient-free switching of the potentiostat and, particularly in the case of macro-scale electrolyses, an instrument with fast overload recovery characteristics. The large initial currents frequently encountered may cause temporary voltage limiting in the potentiostat, and rapid recovery from this condition is desirable. Many operational amplifiers, especially some chopper-stabilized types, are unsuitable for potentiostats without bounding circuits because of very slow (1–2 minute) recovery from saturation. Figure 7 shows the output behavior of the potentiostat as it was switched to operate in the determination of gold in the platinum electrode cell. The large initial current of about 300 mA causes the output to limit for about 2 milliseconds at 24 V, but there is rapid recovery when the maximum available voltage is no longer needed.

The zero offset voltage of the potentiostat is the sum of the offsets of the P85AU voltage follower and the P2A control amplifier. With ±2° C ambient laboratory temperatures, the potentiostat zero offset has remained within ±1 mV for 1 year without readjustment.

Integrator. Because of the long integration times involved, an integrator for controlled-potential coulometer must be extremely stable. The characteristics of most practical interest are the zero drift rate of the integrator output, the day-to-day change in the drift rate, and the ability of the circuit to hold the integral. The instrument described here can be easily adjusted to a zero drift rate of 0.2 mV/15 minutes; the change in the drift rate without readjustment of the balance control, measured after instrument warmups of 0.5 hour, has been less than 0.5 mV/15 minutes in 1 month. The integral holding capability apears to be virtually determined by the zero drift rate of the circuit; thus a voltage of 9.999 V can be held within 0.001 V for 15 minutes. These specifications are well within the tolerances required by most analytical work.

Analytical Determinations. Table II summarizes the results of several different determinations carried out with the controlled-potential coulometer. These were selected from published procedures to demonstrate analyses with two types of cells, both oxidation and reduction processes, and two levels of quantity determined. The low-level uranium analyses were carried out with the 1.9-coulomb full-scale range of the instrument.

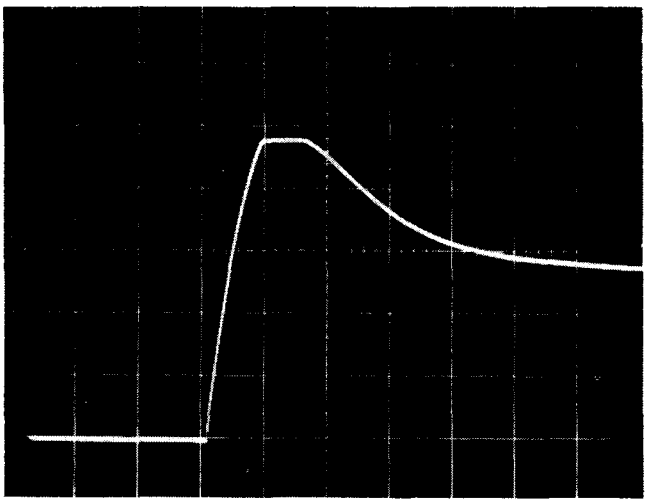

Figure 7. Potentiostat output voltage overload characteristic

Vertical scale: 5 V/division
Horizontal scale: 2 milliseconds/division

Construction Details and Checkout of Instrument. For those who may wish to fabricate the instrument, large-scale wiring and mechanical layout diagrams and a checkout procedure are available from the authors. In addition to the prototype instrument which was built in this laboratory, two units have been fabricated commercially.

RECEIVED for review February 10, 1967. Accepted July 3, 1967. Presented at the Pittsburgh Conference on Analytical Chemistry and Applied Spectroscopy, March 1967. Work performed under the auspices of the U. S. Atomic Energy Commission.